Distinct developmental phenotypes result from mutation of Set8/KMT5A and histone H4 lysine 20 in *Drosophila melanogaster*

Aaron T. Crain[1,3], Stephen Klusza[2,3,8], Robin L. Armstrong[1,3], Priscila Santa Rosa[4], Brenda R. S. Temple[3,5] Brian D. Strahl[1,2,5], Daniel J. McKay[1,3,6,7], A. Gregory Matera[1,2,3,6,7,*], and Robert J. Duronio[1,2,3,6,7,*]

[1]Curriculum in Genetics and Molecular Biology, [2]Lineberger Comprehensive Cancer Center, [3]Integrative Program for Biological and Genome Sciences, [4]UNC PREP, [5]Department of Biochemistry and Biophysics, [6]Department of Biology, [7]Department of Genetics, University of North Carolina, Chapel Hill, NC, 27599 USA

*Corresponding authors

[8]Current address: Department of Biology, Clayton State University, Morrow, GA 30260 USA

Abstract

Mono-methylation of histone H4 lysine 20 (H4K20me1) is catalyzed by Set8/KMT5A and regulates numerous aspects of genome organization and function. Loss-of-function mutations in *Drosophila melanogaster Set8* or mammalian *KMT5A* prevent H4K20me1 and disrupt development. Set8/KMT5A also has non-histone substrates, making it difficult to determine which developmental functions of Set8/KMT5A are attributable to H4K20me1 and which to other substrates or to non-catalytic roles. Here, we show that human KMT5A can functionally substitute for Set8 during *Drosophila* development and that the catalytic SET domains of the two enzymes are fully interchangeable. We also uncovered a role in eye development for the N-terminal domain of Set8 that cannot be complemented by human KMT5A. Whereas $Set8^{null}$ mutants are inviable, we found that an R634G mutation in the SET domain predicted to ablate catalytic activity resulted in viable adults, suggesting important non-catalytic functions of Set8. Similarly, flies that were engineered to express only unmodifiable H4 histones ($H4^{K20A}$) can also complete development, but they are phenotypically distinct from $H4^{K20R}$, $Set8^{null}$, and $Set8^{R634G}$ animals. Taken together, our results demonstrate functional conservation of KMT5A and Set8 enzymes, as well as distinct roles for Set8 and H4K20me1 in *Drosophila* development.

Introduction

The formation of chromatin from DNA and histones regulates genome function and is critical for development of multicellular organisms. The post-translational modification (PTM) of histone N-terminal tails modulates the organization of chromatin and thereby helps regulate replication, repair, and transcription of the genome.[69] Consequently, dysregulation of histone PTMs is thought to disrupt animal development. However, our understanding of how particular histone PTMs influence specific developmental processes is incomplete. For instance, methylation of histone H4 lysine 20 (H4K20me) has been implicated in the control of transcription,[2,9,14,17,38–40,43,44,46,78,90,97,99,105] DNA replication and repair,[9,12,14,26,32,34,42,79,100] chromosome condensation during mitosis,[9,14,16,40] and heterochromatin assembly,[9,14,61,79,84] but the requirement for these putative H4K20me functions has not been directly interrogated during animal development.[49]

In most animal genomes, H4K20 mono-methylation (H4K20me1) is catalyzed by a conserved enzyme variably termed KMT5A/Set8/SETD8/PR-Set7 that contains a catalytic SET domain.[27,61] Subsequent di- and tri-methylation of H4K20 is carried out by SET domain-containing Suv4-20 enzymes, of which there are two in mammals and one in *Drosophila*.[9,71,74,92,98] Developmental roles for H4K20me are typically investigated by mutations that eliminate or alter the activity of these enzymes. Although most of this work has been done using knockdown methods in cell culture,[2,8,16,17,33,34,36,37,62,64,67,70,80,81,85,86,89,97] a small number of studies were conducted using mutant animals.[7,27,40,44,63,72,75] For instance, loss of the H4K20me2 methyltransferase Suv4-20h1 in mice causes early developmental defects, resulting in either embryonic or perinatal lethality.[75] In contrast, animals that lack the H4K20me3 methyltransferase Suv4-20h2 develop normally.[75] *Drosophila Suv4-20* null mutations display no overt developmental defects, suggesting no essential requirement for H4K20me2 and

H4K20me3 in flies.[71] In contrast, loss of H4K20 mono-methyltransferases causes severe developmental phenotypes: Fly *Set8 (*FlyBase annotation *PR-Set7; CG3307)* and mouse *KMT5A* null mutants are inviable and exhibit a developmental arrest that is accompanied by reduction of H4K20me and a variety of defects including smaller larval tissues in flies and increased apoptosis in mouse embryos.[34,40,63,72] Mutant cells also have defects in cell cycle progression and accumulate DNA damage.[9,14,95] These cellular and developmental defects have been attributed to loss of downstream functions that require H4K20 methylation. Consistent with this interpretation, a KMT5A R265G mutation predicted to abolish catalytic activity does not support embryonic development,[63] suggesting that KMT5A catalytic activity is required for proper mouse development.

Each of these analyses is confounded by observations that Set8-family enzymes have protein substrates in addition to H4K20.[23,34,76,83] Moreover, many of these other substrates, such as p53 and PCNA (Proliferating Cell Nuclear Antigen), regulate critical aspects of genome function.[23,76,83,93] Finally, recent work from our group using engineered *Drosophila* histone mutant genotypes demonstrated that H4K20 is dispensable for DNA replication and organismal viability.[49] Thus, the contributions of H4K20me to animal development are not fully determined.

Here, we compare phenotypes caused by mutation of *Set8* and *H4K20* in *Drosophila*. The data show that the essential function played by Set8 in fly development is either non-catalytic or is largely independent of its histone H4K20 methylation activity. We also demonstrate that human KMT5A can functionally substitute for loss of Set8 in *Drosophila*, indicating that flies can provide critical information about evolutionarily conserved functions of H4K20 mono-methyltransferases during development.

Results

Set8 is the appropriate designation for the *Drosophila* H4K20 mono-methyltransferase

The *Drosophila melanogaster* genome encodes fourteen SET [Su(var)3-9, Enhancer-of-zeste, Trithorax] domain lysine methyltransferases (FlyBase)[24,35,56,57,74,77] (Figure 1). A related family of proteins, called PRDMs, is characterized by the presence of a PR domain [PRDF1 (positive regulatory domain I-binding factor 1) and RIZ1 (retinoblastoma protein-interacting zinc finger gene 1)] along with a variable number of Cys2-His2 (C2H2) zinc fingers.[88] The PR domain is an evolutionarily recent subtype of the SET domain, although not all PRDMs encode active methyltransferases.[88] There are four PRDM proteins (Blimp-1, Hamlet, CG43347, Prdm13) in insect genomes whereas this family has expanded to nineteen proteins in humans.[29,48,88]

In *Drosophila,* the protein encoded by *PR-Set7/CG3307* is orthologous to the human H4K20 methyltransferase SETD8/KMT5A and it neither contains a PR domain nor any predicted zinc finger motifs[15,27,61] (Figure 1). In contrast, human PRDM7 (PR/SET Domain 7) is an H3K4 methyltransferase that is most closely related to the KRAB and Zn finger domain protein, PRDM9[10] (Figure 1). Moreover, human SETD7/Set7/Set9 is yet another human H3K4 methyltransferase[91] distinct from *Drosophila* PR-Set7/CG3307 (Figure 1). To avoid further confusion, we propose to officially rename *CG3307* as *Set8* and refer to this protein as Set8 throughout the manuscript.

Human KMT5A rescues loss of Set8 in *Drosophila*

KMT5A and Set8 are essential for the development of mice and flies, respectively, and mutating these enzymes results in defects in cell cycle progression, DNA damage response, and chromatin compaction in both organisms.[40,63,70] The SET domains of Set8 and human KMT5A are 57% identical (Supplemental figure 1). Therefore, we hypothesized that KMT5A and Set8 perform the

same biological functions in *Drosophila* and mammals and that human KMT5A would rescue loss of Set8 in *Drosophila*. To test this hypothesis, we engineered a *KMT5A* open reading frame that was codon-optimized for translation in *Drosophila* and expressed in the context of the native *Set8* gene (a 4774 bp genomic fragment including 1325 bp upstream of the ORF and 2021 bp downstream of the ORF including both native 5' and 3' UTRs). Using this engineered *KMT5A* allele, we generated transgenes located on the same chromosome as the $Set8^{20}$ null allele[40] (Figure 2A). Whereas $Set8^{20/20}$ mutants die as early pupae, animals expressing KMT5A in a $Set8^{20/20}$ background pupate normally and complete development at similar frequencies as wild type animals or $Set8^{20/20}$ animals rescued with a control *Set8* transgene (Figure 2B, C). Although $Set8^{20/20}$ animals rescued by KMT5A are viable and fertile, we observed a rough eye phenotype in 58% of adult flies (Figure 2E). The *Drosophila* compound eye is a highly organized tissue containing ~800 photoreception structures termed ommatidia, each composed of eight photoreceptor neurons and a set of accessory cells. Many processes contribute to proper formation of the adult eye, including cell cycle progression, cell death, and ultimately cell differentiation. Disruption of any one of these processes can contribute to ommatidial irregularities that manifest as a visible "roughness" of the adult eye.[6,94] Even subtle defects in gene functions required for eye development can result in rough eyes, and thus we conclude that KMT5A fully rescues most, but not all, Set8 functions in *Drosophila*.

The N-terminus of Set8 is dispensable for *Drosophila* viability but plays a role in eye development

Although the SET domains of Set8 and KMT5A are 57% identical, the full-length proteins are only 21% identical (Supplemental figure 1). The N-terminal region (554aa) of Set8 is predicted to be largely unstructured and is not well-conserved with KMT5A (Figure 2A). A multiple

protein alignment of 301 BLAST hits with greater than 50% identity to the full-length Set8 protein revealed that this N-terminal region of Set8 is unique to flies (order Diptera), whereas the SET domain is highly conserved across all represented organisms (Figure 2D). To test whether the N-terminal region of Set8 functions in *Drosophila* development we engineered a transgene encoding a Set8 protein lacking the first 339 amino acids ($Set8^{\Delta N}$), which would produce a protein the size of KMT5A (Figure 2A). The $Set8^{\Delta N}$ transgene rescued $Set8^{20/20}$ lethality resulting in fully viable and fertile adults with a highly penetrant (82%) rough eye phenotype (Figure 2B, C, E). Although we were unable to assess the protein accumulation of $Set8^{\Delta N}$ because the epitope recognized by the Set8 antibody is within the N-terminal region, these results indicate that the N-terminal 339 amino acids are dispensable for normal development except in the eye. To test whether the eye function could be provided by KMT5A, we generated a chimeric transgene with the Set8 N-terminus (1-554) fused to the KMT5A C-terminus (N-Set8::KMT5A-C) and a reciprocal chimeric transgene with the KMT5A N-terminus (1-214) fused to the Set8 C-terminus (N-KMT5A::Set8-C). Both transgenes fully rescued viability and fertility of $Set8^{20/20}$ mutants (Figure 2 B, C). Further, *N-KMT5A::Set8-C* animals displayed a rough eye phenotype like *KMT5A* and $Set8^{\Delta N}$ animals (Figure 2E). By contrast, flies expressing the *N-Set8::KMT5A-C* chimera were fully viable and fertile with morphologically normal eyes, indicating the human KMT5A SET domain is functionally equivalent to that from *Drosophila* Set8 (Figure 2B, C). We conclude that the N-terminal 339 amino acids of Set8 are dispensable for *Drosophila* viability and fertility but have a function in eye development that cannot be provided by the first 214 amino acids of human KMT5A.

A SET domain mutation predicted to block methyltransferase activity does not result in a Set8 null phenotype

Many of the established roles for the KMT5A/Set8 lysine methyltransferase have been attributed to its catalytic activity, primarily by using cell culture-based assays.[2,8,16,17,33,34,36,37,62,64,67,70,80,81,85,86,89,97] To determine whether methyltransferase activity is required for Set8 function during *Drosophila* development, we engineered point mutations in the SET domain that are predicted to ablate catalytic activity[27,61] (Figure 3A). SET domains are highly conserved and contain evolutionarily invariant residues within the catalytic core (Figure 3B). As shown in Figure 3C, two of these residues (R634 and H638) make critical contacts with the methyl donor, S-adenosyl methionine (SAM). Mutation of the homologous Arg residue in the human enzyme (R265) to Gly blocks methyltransferase activity *in vitro* using nucleosomal substrates, and this substitution has been used in numerous studies of Set8/KMT5A proteins to create catalytically inactive enzymes.[1,2,17,26,33,38,61,63,76,80,84,86,96] We therefore engineered a $Set8^{R634G}$ mutation (hereafter $Set8^{RG}$) in the context of the rescuing genomic fragment used in the experiments above. We also engineered an R634G, H638L double mutation (hereafter $Set8^{RGHL}$). Using *in silico* structural models based on the solved human KMT5A structure and molecular dynamics simulations (Figure 3C), each of these amino acid changes were evaluated for their impact on SAH binding and H4 peptide binding. While H4 peptide binding was minimally impacted, the mutations were shown to disrupt SAH binding and thus are predicted to reduce or eliminate methyltransferase activity of the mutant Set8 proteins (Figure 3C, D).

We inserted $Set8^{RG}$ and $Set8^{RGHL}$ transgenes into the same chromosomal landing site used for the KMT5A rescue experiments (Figure 2A). We then assessed expression of these transgenes in a $Set8^{20/20}$ background by immunoblot analysis of third instar larval brain extracts.

As demonstrated previously, there is no detectable Set8 protein in *Set8*$^{20/20}$ homozygous null mutant animals[40] (Figure 3E). The Set8(RGHL) mutant protein accumulates to about 10% of Oregon-R wild-type control (Figure 3E, F), suggesting that binding of the SAM cofactor stabilizes Set8 protein. Consistent with this result, *Set8*^{RGHL} animals are phenotypically similar to *Set8*$^{20/20}$ null mutants, arresting development as early pupae (Figure 4A, B). Interestingly, *Set8*^{RGHL} wandering larvae accumulate melanotic masses that we did not observe in *Set8*^{null} animals. This phenotype is associated with immune response and was previously reported to be variably expressive and penetrant in both *Set8*^{20} and *Set8*^{1}*/Df(3R)red3l* animals.[55] In contrast, levels of the Set8(RG) missense protein are comparable to those of wild type Set8 expressed from a control *Set8*^{WT} transgene (Figure 3E, F), indicating that the R634G mutation does not impact protein stability. The *Set8*^{RG} transgene rescues the early pupal lethality observed in *Set8*$^{20/20}$ mutants, but only ~50% of the *Set8*^{RG} animals eclose as adults compared to the *Set8*^{WT} control (Figure 4A, B). A majority of *Set8*^{RG} mutant flies had rough eyes (86%, Figure 4C), as was previously shown for flies harboring the *Set8*^{1} hypomorphic mutation, which is caused by a P-element insertion in the 5'-UTR.[27,40,61] *Set8*^{RG} also behaves as a hypomorphic allele, as animals containing two *Set8*^{RG} transgenes have a less severe phenotype than those containing one (Figure 4B). These data indicate that the *Set8*^{RG} allele is not null, and thus Set8(RG) protein retains at least some Set8 function *in vivo*.

To further characterize the *Set8*^{RG} mutant, we more closely evaluated the process of pupariation in our collection of *Set8* mutants. Easily recognizable developmental events occur during the larval to pupal transition in *Drosophila,* including eversion of the anterior spiracles and gas bubble translocation from the posterior to anterior end of the pupa. Whereas S*et8*$^{+/20}$ heterozygotes and *Set8*$^{1/20}$ hypomorphs progress normally through these developmental

milestones, $Set8^{20/20}$ mutants fail to complete both anterior spiracle eversion and gas bubble translocation, resulting in pupae with increased length compared to control and $Set8^{1/20}$ hypomorphs (Figure 4D). $Set8^{RG}$ animals displayed a slight defect in completion of these pupariation events compared to $Set8^{WT}$ control animals. Pupariation defects observed in $Set8^{RGHL}$ animals were like those in $Set8^{20/20}$ mutants. Interestingly, $Set8^{RG}$ mutants also displayed a slight increase in pupal length compared to $Set8^{WT}$ controls that did not reach the severity observed in $Set8^{20/20}$ mutants (Figure 4D). These data demonstrate that the SET catalytic domain mutant $Set8^{RG}$ displays intermediate pupariation defects between wild type and null alleles of Set8, suggesting that successful completion of the larval to pupal transition may require both catalytic and non-catalytic functions of Set8.

Mutants of H4K20 and Set8 are phenotypically distinct

Mutation of lysine methyltransferases can result in disruption of multi-protein complexes, causing pleiotropic phenotypes independent of histone methylation.[20,31,45,82,87,107] In addition, Set8 has non-histone substrates and non-catalytic functions.[23,26,34,76,80,83,100,108] Thus, one cannot conclusively determine functional roles for H4K20me solely by mutating Set8. Another genetic strategy to address the contribution of H4K20me to various genomic processes is to change H4K20 to a residue that cannot be modified by Set8. However, this genetic strategy is not usually employed in metazoan systems because in these organisms the replication-dependent (RD) histones (H1, H2A, H2B, H3, and H4) are encoded by multiple genes located at different loci, making genetic manipulation extremely difficult. In contrast, in *Drosophila melanogaster* all ~100 replication-dependent histone genes are tandemly arrayed at a single locus that can be removed with a single genetic deletion. The early developmental arrest caused by homozygosity of this deletion can be rescued with a single, ectopic transgene encoding 12 tandemly arrayed

histone wild type gene repeats (HWT; Figure 5A, see Meers et al. 2018[52] for details on array construction). This strategy allows us to engineer histone genotypes encoding mutant histone proteins in which a given residue is changed to one that is not a substrate for its cognate modifying enzyme.[5,41,49–52,65,66]

Using this strategy, we demonstrated previously that $H4^{K20A}$ mutant animals can survive to adulthood[49] (Figure 5C, D). By contrast, 100% of $Set8^{20/20}$ null animals die as larvae or early pupae[40] (Figure 2C). This stark phenotypic difference between $H4^{K20A}$ and *Set8* mutants suggests that certain *Set8* phenotypes might not be due to loss of H4K20me, but rather to loss of methylation of its non-histone substrates or non-catalytic functions. To investigate this disparity further, we first generated $H4^{K20R}$ mutants[52] and compared the resulting phenotypes to those of $H4^{K20A}$ animals as well as of *Set8* mutants. Whereas a fraction of $H4^{K20A}$ mutants can survive to adulthood, we found that all $H4^{K20R}$ mutants fail to eclose as adults, although some reach the pharate adult stage (Figure 5C, D). In addition, $H4^{K20R}$ animals pupate much less frequently than either $H4^{K20A}$ mutants or $H4^{HWT}$ controls. Notably, the $H4^{K20R}$ mutant pupae are much smaller and shorter than either $H4^{HWT}$ control or $H4^{K20A}$ mutant pupae, indicating a growth defect (Figure 5E, F). Despite this defect, we did not detect a change in cell cycle progression by FACS analysis of cells from $H4^{K20R}$ wing imaginal discs (Figure 5B). In contrast, $H4^{K20A}$ cells accumulate in G2 relative to controls, with a concomitant reduction in S phase (Figure 5B). Notably, Set8 deficient cells arrest in G2/M in both flies and mammalian cell culture.[14,40] Taken together with the overall eclosion frequency differences, these data demonstrate that the $H4^{K20R}$ mutation is more severe than the $H4^{K20A}$ mutation developmentally, but that each mutation influences cellular mechanisms in unique ways (See Discussion).

One complication of these studies is that the fruitfly genome contains a single-copy replication-independent H4 gene (*His4r*) on chromosome 3 (i.e., located outside of the RD histone gene array on chromosome 2). *His4r* encodes an H4 protein that is identical to the RD H4[3]. Although this gene is non-essential (Figure 5C, D), we and others have found that His4r can partially compensate for loss of RD H4.[5,19,28,49] Therefore, we used CRISPR-Cas9 to engineer two *His4r* alleles (a deletion[5], $His4r^{\Delta}$ [5] and a K20A mutant, $His4r^{K20A}$) and we combined them with the appropriate RD histone mutant genotypes (Figure 5A). As shown in Figures 5C and D, homozygous loss of *His4r* in an $H4^{K20A}$ background ($H4^{K20A}$, $His4r^{\Delta/\Delta}$) reduces viability, but does not eliminate it, indicating that His4r expression is important for the observed viability of $H4^{K20A}$ mutants but is not required. Expressing one copy of $His4r^{K20A}$ further reduces viability (Figure 5C, D), suggesting a dominant toxicity of the H4K20A protein. In contrast, deleting *His4r* in an $H4^{K20R}$ background did not appreciably change the lethal period of $H4^{K20R}$ animals (Figure 5C, D).

We next compared H4K20 and Set8 mutant phenotypes, focusing on pupariation and eye development. In contrast to $Set8^{20/20}$ null mutants, which display defects during pupariation, >80% of the $H4^{K20A}$ and $H4^{K20R}$ animals complete proper anterior spiracle eversion and gas bubble translocation. Similarly, the viable $Set8^{RG}$ and $Set8^{1/20}$ mutants did not exhibit defects in anterior spiracle eversion or gas bubble translocation. Both $Set8^{RG}$ and $Set8^{1/20}$ mutants have rough eyes[27] (Figure 4C), indicating that Set8 is required for eye development. In contrast, none of the $H4^{K20A}$ mutants had rough eyes when *His4r* was present, whereas ~21% of $H4^{K20A}$, $His4r^{\Delta/\Delta}$ animals only had mild disorganization of interommatidial bristles (Figure 5G). These results suggest that the roles of Set8 and H4K20me in eye development are distinct, and further highlight that the differential effects of Ala and Arg substitutions at H4K20. We conclude that

H4K20me does not mediate all functions of Set8 because mutating H4K20 and Set8 cause different developmental phenotypes.

Discussion

We use genetic and genomic approaches in *Drosophila* to investigate how histone PTMs, and the enzymes that install them, contribute to animal development. It is particularly informative to determine where these contributions differ. Our results indicate that only a subset of the essential functions of the H4K20 mono-methyltransferase, Set8, are mediated by H4K20me. The data also reveal that, although H4K20me is formally dispensable for completion of development, the lysine residue nonetheless plays an important role.

Drosophila Set8 and human KMT5A are orthologous

We showed that human KMT5A can substitute for all Set8 functions during *Drosophila* development, except in the eye, where we observe a minor disruption in ommatidial organization that manifests as a rough eye in *KMT5A*-rescued adults. The eye phenotype likely does not result from changes in methylation of substrates, as we found that the human KMT5A SET domain can fully substitute for that of Set8, even in the eye. Rather, full developmental eye function is instead provided by the non-catalytic amino terminal 339 amino acids of Set8, which is conserved in other Diptera, but not in humans or other vertebrates and invertebrates. Nonetheless, we found that the rough eye phenotype was more penetrant in $Set8^{\Delta N}$-rescued animals than it was in the *KMT5A*-rescued animals. We designed $Set8^{\Delta N}$ to be the same size as KMT5A and retain the conserved PIP degron and Cdk consensus phosphorylation site[96] found in KMT5A, which therefore might provide some function during eye development. Because KMT5A can perform nearly all the biological functions of Set8 in *Drosophila*, studies of Set8

could be applicable to human biology and disease, particularly because aberrant levels of KMT5A are implicated in the development of and increased risk in certain breast, brain, and liver cancers.[18,22,54,59,76,83,97,104,106] KMT5A has also been shown to regulate androgen receptor-mediated transcription in prostate cancer.[99]

Mutation of the SET domain does not abolish *in vivo* function of Set8

Whether methyltransferase activity is required for all the cellular and developmental roles of SET domain proteins remains an open question in the field. This question is generally addressed by testing the *in vivo* function of "catalytically dead" enzymes. Previous *in vitro* studies showed that an R265G mutation eliminates catalytic activity of KMT5A.[60] We found that the corresponding $Set8^{R634G}$ mutation does not cause a null mutant phenotype and supports development into viable adults. This result suggests that methylation of both H4K20 and non-histone substrates of Set8 is not required for completion of development in *Drosophila*. However, we do not know whether $Set8^{RG}$ flies retain some H4K20 methylation. Thus, one possibility is that an enzyme other than Set8 could methylate H4K20 in *Set8* mutant animals, but the levels of H4K20me attained would not provide full biological function. Another possibility is that the $Set8^{RG}$ mutant is a catalytic hypomorph *in vivo*. Consistent with this possibility, the $Set8^{RG}$ mutant phenotype resembles that of the previously described $Set8^{1}$ hypomorphic mutant (viable with rough eyes),[27,40] and we found that two copies of the $Set8^{RG}$ transgene provide more function than one copy, indicating that $Set8^{RG}$ is a genetic hypomorph. In addition, our structural analyses revealed that R634G disrupts interactions within the SAM binding domain but does not eliminate the possibility that SAM and K20 might still occupy the active site of the enzyme, albeit less avidly. Notably, other studies have concluded that catalytic activity is not required for

in vivo function of the H3K4 mono-methyltransferase (Mll3/4, Trr).[25,68] Thus, critical non-catalytic roles of histone methyltransferases may be the norm rather than the exception.

Comparative genetic analyses support distinct developmental roles for Set8 and H4K20me

Our analysis of H4K20 mutants is consistent with the idea that Set8 provides essential functions during metazoan development that do not include H4K20 methylation. Animals entirely lacking H4K20me (*H4*^{K20A}*, His4r*$^{\Delta/\Delta}$ and *H4*^{K20A}*, His4r*$^{K20A/\Delta}$) can develop into adults with no obvious morphological defects, whereas all animals lacking the H4K20 methyltransferase (*Set8*$^{20/20}$) die in early pupal stages. This difference in phenotype supports the hypothesis that *Set8*$^{20/20}$ inviability is due, at least in part, to loss of non-histone substrate methylation and/or non-catalytic functions of Set8. Nevertheless, H4K20 is clearly quite important, as only a small fraction of *H4*^{K20A} mutants complete development and *H4*^{K20R} mutants are inviable. Moreover, ectopic expression of H4K20A mutant histones in cultured human cells supports a role for H4K20me in S phase progression, particularly in late replicating heterochromatin.[13]

The phenotypic differences we observe between *H4*^{K20A} and *H4*^{K20R} mutants are intriguing, as both substitutions are expected to eliminate H4K20me. The differences may well be attributable to idiosyncratic structural properties of H4A20- vs. H4R20-containing nucleosomes, relative to wild type. In particular, the side chains of Alanine and Arginine differ in both size and charge and thus may differentially impact interaction of the H4 tail with chromatin binding complexes irrespective of H4K20 methylation. For instance, proteins that bind unmethylated H4K20 (BRCA1-BARD1) do not recognize H4K20A nucleosomes.[58] Given the proximity of H4K20 to the nucleosome core, these mutations may variably influence chromatin structure, or affect the modification of other residues on the H4 tail or on other histones within the nucleosome. Notably, the assumption that a Lys for Arg substitution would be less

detrimental than a Lys for Ala substitution (because Lys and Arg have a similar side chain structure and are both positively charged) is not born out by our data. Regardless of the precise mechanism, our genetic analyses provide important insight into H4K20me function *in vivo*, and suggest that future biochemical, proteomic, and ultrastructural studies of these histone mutants will be informative.

Materials and Methods

Fly stocks and husbandry

Fly stocks were maintained on standard corn medium with molasses provided by Archon Scientific (Durham). The $Set8^{20}$ stock used in this study was a generous gift from Ruth Steward. The $Set8^{1}$ (#10278) stock was obtained from the Bloomington Stock Center.

Set8, KMT5A, and chimeric transgenes

For the $Set8^{WT}$ transgene a 5493 bp genomic fragment was amplified from a wild type fly extract using the following primers 5' acttatacacttcattcct 3' and 5' tacccgcctgatgcgaattt 3'. The genomic fragment was cloned into pDEST w+ attB (Supplemental Figure 2). $Set8^{RG}$ and $Set8^{RGHL}$ were constructed using site-directed mutagenesis using the Q5 Site-directed Mutagenesis kit on pDEST w+ attB $Set8^{WT}$ (NEB E0554S). KMT5A, $Set8^{\Delta N}$, N-KMT5A::Set8-C, and N-Set8::KMT5A-C sequences were synthesized using GENEWIZ gene synthesis (Supplemental Figure 3) and cloned into pDEST w+ attB digested with AgeI and MluI (Supplemental Figure 2). Transgenes were sequence-verified and injected into VK33 on chromosome 3L and screened for positive transformants by BestGene. Recombinant flies were generated by crossing transgenic flies with flies containing $Set8^{20}$ and screening single F2 male progeny for the presence of both the appropriate transgene and $Set8^{20}$.

Western blots

Twenty brains from third instar wandering larvae of each genotype were collected in 1xPBS (137 mM NaCl, 2.7 mM KCl, 10 mM Na_2HPO_4, 1.8 mM KH_2PO_4). 1xPBS was removed, 100 uL of RIPA buffer (50 mM Tris pH 7.5, 0.1% SDS, 0.5% Sodium Deoxycholate, 1% NP-40, 150 mM NaCl, 5 mM EDTA)) was added to each sample. Larvae were homogenized in RIPA buffer using a pestle and incubated on ice for 30 minutes. Samples were then centrifuged for 15 minutes at top speed at 4C. Supernatant was separated from pellet and protein concentration was assessed using a Bradford assay. Then 4x Laemmli sample buffer (BioRad 1610747) with 10% β-mercaptoethanol was added to each sample at a 3:1 ratio. Samples were boiled for 10 minutes and equal protein (~10 ug) was loaded on a 12% SDS-PAGE gel. Proteins were transferred to a 0.45nm nitrocellulose membrane for 60 minutes at 100V. Membranes were blocked with 5% milk in 1xTBS-Tween (10mM Tris, 150 mM NaCL, 0.1% Tween20) for 60 minutes then blotted with primary antibodies (Set8: Novus Biologicals 44710002; β-tubulin: Abcam ab6046) in 5% milk in 1xTBS-Tween overnight. Blots were quickly washed 3x then for 10 minutes 3x. Blots were incubated with secondary antibody (goat anti-Rabbit) in 5% milk in 1xTBS-Tween for two hours at room temperature. Blots were again quickly washed 3x then for 10 minutes 3x. Blots were then incubated with SuperSignal™ West Pico PLUS Chemiluminescent Substrate (Thermo Scientific 34580) and imaged using a GE Amersham Imager. Quantification was performed using FIJI. Briefly, the signal of each band on the Set8 blot and β-tubulin blot was quantified using a box of equal area. Signal from $Set^{20/20}$ was subtracted from each Set8 value, then divided by the corresponding β-tubulin signal for each lane. Finally, the value of *Oregon-R* was set to 1, so values of all other genotypes are relative to that genotype.

Viability assays

To investigate the requirement of Set8 and H4K20me for organismal viability, we enriched cultures of each genotype for 1st instar larvae by manually separating them from their wild type siblings and monitored survival to pupal and adult developmental stages. Mean pupation and adult values and pairwise comparisons for each genotype can be found in Supplemental Figure 4. Crosses to generate histone mutant genotypes were the same as previously reported.[4,52]

CRISPR for *His4r*

The *His4rΔ* allele utilized in this study was the same generated by Armstrong et al. 2018. Here we generated a point mutation allele (*His4r*^{K20A}) using CRISPR-Cas9 mutagenesis. The genomic region including *His4r* was amplified using the following primers 5'-gctgcgccgttagataaagc-3' and 5'-agcaatcggagtccatg-3' and TOPO cloned in pENTR. The codon for His4r^{K20} was changed to Ala using the Q5 Site-directed Mutagenesis kit (NEB E0554S). The same gRNA constructs in pCFD3 from Armstrong et al. 2018 were co-injected with the K20A-mutated *His4r* repair construct into *Drosophila* embryos expressing Cas9 from the nanos promoter. Positive hits were screened using a BbsI site created by the Lys to Ala mutagenesis.

Scanning electron microscopy

Flies were deyhydrated in ethanol and images of compound eyes were taken using a Hitachi TM4000Plus table top SEM microscope at 10kV and 150x magnification.

FACS

Wing imaginal disc nuclei from third instar wandering larvae of each genotype were sorted into G1, S, and G2 populations by a FACSAria II or III based on DAPI intensity as previously described.[5,53]

Protein sequence analyses

Figure 1A: PRDM and SET domain methyltransferase protein sequences (Supplemental Figure 5) were compiled and aligned with ClustalOmega using the msa package.[11] A distance matrix was calculated by identity using dist.alignment in the seqinr package. A phylogenetic tree based on the distance matrix was generated and then plotted using ggtree.[101–103]

Figure 2C: The full-length *Drosophila melanogaster* Set8 protein sequence was BLASTed against the refseq_protein database using the default parameters. The top 1000 hits were compiled and manually sorted to include only one protein isoform per organism. Proteins with percent identities to the full-length *Drosophila melanogaster* Set8 less than 50% were discarded. Human and mouse KMT5A proteins were retained for downstream analysis despite having percent identities lower than 50%. The remaining protein sequences (Supplemental Figure 6) were aligned with ClustalOmega from the msa package.[11] Phylogenetic classification of each protein was performed with the taxize package and merged with the alignment information. Proteins with incomplete classification information were discarded. A phylogenetic tree was generated using the classification information and plotted using ggtree.[101–103] The alignment of all remaining proteins was plotted in order of the phylogenetic tree and each position in the alignment was colored based on whether it matched the residue in the corresponding position of Drosophila melanogaster Set8 (blue), Human KMT5A (pink), both *Drosophila melanogaster* Set8 and KMT5A (maroon), or

neither *Drosophila melanogaster* Set8 and KMT5A (black). Gaps in the alignment are represented by white space.

Molecular dynamics simulations

Structural models of *Drosophila* WT and mutant Set8/KMT5A in ternary complexes with SAH (S-adenosyl-L-homocysteine) and H4 peptide were built using the crystallographic structure of human KMT5A in ternary complex (PDB ID: 1zkk) [PMID 15933070] as template. These structural models were then used as starting structures for molecular dynamics simulations. Four replicate explicit solvent simulations with the same starting conformations but different velocity distributions were completed for WT and each mutant using the Amber v18 software package.[21] LEaP from the Amber software package was used to generate the explicit solvent systems in an octahedral box with charge neutralization while the GPU version of PMEMD was used to complete the simulations.[30,73] The ff14SB force field was used for parameterization.[47] A total of 5,000 steps of minimization were completed, followed by 500 psec heating with an NVT ensemble, and then density equilibration over 500 psec with an NPT ensemble. The production run was in the NPT ensemble for a total of 500 nsec. During the production run, Langevin dynamics with a collision frequency of 1.0 $psec^{-1}$ was used for temperature regulation. A Berendsen barostat with a relaxation time of 1.0 psec was used for pressure regulation. The time-step was 2 fsec with hydrogen atoms constrained by SHAKE. Trajectories were analyzed for the distance between atoms in Set8/KMT5A and atoms in either the H4 peptide or SAH.

Full genotypes of strains used in this study.

$Set8^{WT}$: *y-w-;;{*$Set8^{WT}$*}*, $Set8^{20/20}$

$Set8^{RG}$: *y-w-;;{*$Set8^{RG}$*}*, $Set8^{20/20}$

$Set8^{RGHL}$: *y-w-;;{*$Set8^{RGHL}$*}*, $Set8^{20/20}$

441 *KMT5A: y-w-;;{KMT5A}, $Set8^{20/20}$*

442 *$Set8^{\Delta N}$: y-w-;;{$Set8^{\Delta 1\text{-}339}$}, $Set8^{20/20}$*

443 *N-KMT5A::Set8-C: y-w-;;{$KMT5A^{1\text{-}214} – Set8^{555\text{-}691}$}, $Set8^{20/20}$*

444 *N-Set8::KMT5A-C: y-w-;;{$Set8^{1\text{-}554} – KMT5A^{215\text{-}352}$}, $Set8^{20/20}$*

445 *HWT: y-w-; ΔHisC; {12xHWT}*

446 *HWT, $His4r^{\Delta/\Delta}$: y-w-; ΔHisC; {12xHWT}, $His4r^{\Delta/\Delta}$*

447 *$H4^{K20A}$: y-w-; ΔHisC; {12x$H4^{K20A}$}*

448 *$H4^{K20R}$: y-w-; ΔHisC; {12x$H4^{K20R}$}*

449 *$H4^{K20A}$, $His4r^{\Delta/\Delta}$: y-w-; ΔHisC; {12x$H4^{K20A}$}, $His4r^{\Delta/\Delta}$*

450 *$H4^{K20A}$, $His4r^{K20A/\Delta}$: y-w-; ΔHisC; {12x$H4^{K20A}$}, $His4r^{K20A/\Delta}$*

451 *$H4^{K20R}$, $His4r^{\Delta/\Delta}$: y-w-; ΔHisC; {12x$H4^{K20R}$}, $His4r^{\Delta/\Delta}$*

452 **Data availability**

453 Strains and plasmids available upon request. The authors affirm that all data necessary for

454 confirming the conclusions of the article are present within the article, figures, and tables.

455 **Acknowledgements**

456 A.T.C. and R.L.A. were supported in part by NIH predoctoral traineeships, T32-GM007092. S.K. was
457 supported in part by an NIH diversity supplement to grant R01-DA036897 (to R.J.D., A.G.M. and B.D.S.)
458 and by a postdoctoral traineeship, T32-CA009156. This work was supported by NIH grants R35-
459 GM136435 (to A.G.M) and R01-GM124201 (to R.J.D.). We thank Ruth Steward for generously
460 providing fly stocks and Megan Butler for critical reading of the manuscript.

461 **Figure Legends**

462 **Figure 1. Evolutionary relationship of *Drosophila* and human SET and PRDM containing**
463 **proteins**. Unrooted tree produced from an alignment of human and *Drosophila* PRDM and SET
464 domain family proteins using ClustalOmega. *Drosophila* proteins are indicated with bold,

underlined text. The red oval highlights the grouping of SET domain family proteins, including PR-Set7/Set8 and KMT5A (white).

Figure 2. Human KMT5A functionally substitutes for Set8 during *Drosophila* development. A) Diagram of Set8, KMT5A, and Set8/KMT5A chimeric proteins expressed from transgenes located on chromosome 3, which also contains the $Set8^{20}$ null allele. Red shading and non-bold, non-italic numbers indicate Set8 sequence. Gray shading and bold, italic numbers indicate KMT5A sequence. In parentheses is the total number of amino acids in each protein product. B) Pupation of $Set8^{WT}$, *KMT5A*, and chimera genotypes. Each circle represents the percentage of 40-50 larvae in a vial that reached pupation. The mean and standard deviation of these percentages for 8-10 vials are shown for the indicated genotypes. All transgenic genotypes are in the $Set8^{20/20}$ homozygous null background. "2x" indicates that each transgene is also homozygous. C) Eclosion into adults of $Set8^{WT}$, *KMT5A*, and chimera genotypes. Here, each circle represents a vial of 40-50 larvae, and 8 vials for each of the indicated genotypes were scored. Genotypes are as in panel B. D) Annotated alignment of Set8-related proteins. 301 homologous proteins with over 50% identity to Set8 as identified via BLAST were aligned using Clustal Omega and ordered by phylogeny. Set8 and KMT5A schematics are shown at the top of the diagram with the SET domains indicated by dark blue boxes. Residues of each protein in the alignment that match both Set8 and KMT5A exactly are colored dark red. Those that match only Set8 are colored light blue, and those that match only KMT5A are colored pink. Residues that match neither are colored black. Gaps in the alignment are indicated by white space. E) SEM images of adult eyes of flies of the indicated genotypes. The penetrance of flies displaying a phenotype like that shown is indicated below each image. "1x" and "2x" indicate flies containing either 1 or 2 copies, respectively, of the transgene expressing Set8, KMT5A, or Set8/KMT5A chimeras in the $Set8^{20/20}$ homozygous null background.

Figure 3. Generation Set8 proteins predicted to be catalytically inactive.

A) Diagram of Set8(WT), Set8(RG) and Set8(RGHL) proteins expressed from transgenes located on chromosome 3. B) Conservation of the Set8 Arg634 and Leu638 residues (orange bars) among KMT5A proteins from human, frog, and sea urchin, and among other SET domain proteins from these species. Asterisks mark where residues are identical across all twelve proteins. C) Modeling of Set8 with SAH and peptide from H4 bound to the enzyme. Shown are representative structures after 500ns of molecular dynamics for Set8, Arg634Gly and Arg634Gly, His638Leu mutations in Set8. D) Total length of time during 500 ns simulations that ligands remained in binding pocket as measured by distances between key atoms. The two distance measurements shown were selected because they were the most stable interactions between Set8 and H4 peptide and between Set8 and SAH. The selected hydrogen bond to the peptide was also the most stable interaction with the peptide and one of the last to be broken. Circles represent values from four replicate simulations. E) Western blot of third instar larval brain extracts from Oregon R wild type and the indicated Set8 mutants using anti-Set8 and anti-

β-tubulin antibodies. F) Quantification of anti-Set8 signal on western blots by densitometry (see methods). Shown is the mean and standard deviation of measurements (circles) from technical replicates across four biological replicates. Oregon-R normalized signal was set to 1 for each replicate. Significance was determined by a one-way Anova followed by Tukey's multiple comparison test. **** indicates p<.0001 and ns indicates not significant.

Figure 4. The *Set8^{RG}* mutant phenotype is not null.

A) Pupation and B) Eclosion into adults of *Set8^{RG}* and *Set8^{RGHL}* mutants. Each circle represents the percentage of 40-50 larvae in a vial that reached pupation or adulthood. The mean and standard deviation of these percentages for 8 vials are shown for the indicated genotypes. Note that the Oregon R and *Set8$^{20/20}$* data in panels A and B are identical to Figure 2B and 2C, respectively, and shown here to allow comparison. C) SEM images of adult eyes of flies of the indicated genotypes. Penetrance and transgene copy number are as in Figure 2 legend. D) Pupal length was measured for animals of the indicated genotypes. Each symbol represents a single pupa. Thick bar indicates the mean and thin bars indicate standard deviation. ns indicates not significant and **** indicates $p < 0.0001$ by Student's t test.

Figure 5. H4K20 mutant phenotypes differ from Set8 mutant phenotypes.

A) Diagram of histone mutant genotypes. A deletion of HisC on the second chromosome is rescued by a third chromosome containing a transgenic 12x histone gene arrays and either with or without a mutation of *His4r*. B) FACS analysis of DNA content within cells obtained by dissociation of larval wing imaginal discs. The percentage of cells in each phase of interphase is shown for the indicated genotypes. C) Pupation and D) eclosion into adults of different H4 mutants. Each circle represents the percentage of 40-50 larvae in a vial that reached pupation or adulthood. The mean and standard deviation of these percentages for 8-11 vials are shown for the indicated genotypes. E) Pupal length was measured for animals of the indicated control and H4 genotypes. Each symbol represents a single pupa. Thick bar indicates the mean and thin bars indicate standard deviation. ** indicates p<0.004 and **** indicates $p < 0.0001$ by Student's t test. F) Representative image used for the pupal length data in panel E. G) SEM images of adult eyes of flies of HWT control and the indicated H4 mutant genotypes. Rough eye phenotype penetrance is indicated below each image.

References

1. Abbas T, Mueller AC, Shibata E, Keaton M, Rossi M, Dutta A. CRL1-FBXO11 promotes Cdt2 ubiquitylation and degradation and regulates Pr-Set7/Set8-mediated cellular migration. Molecular Cell.

2013 [accessed 2021 May 3];49(6):1147–1158. https://pubmed.ncbi.nlm.nih.gov/23478445/. doi:10.1016/j.molcel.2013.02.003

2. Abbas T, Shibata E, Park J, Jha S, Karnani N, Dutta A. CRL4Cdt2 Regulates Cell Proliferation and Histone Gene Expression by Targeting PR-Set7/Set8 for Degradation. Molecular Cell. 2010 [accessed 2019 Jul 24];40(1):9–21. https://www.sciencedirect.com/science/article/pii/S1097276510007422?via%3Dihub. doi:10.1016/J.MOLCEL.2010.09.014

3. Akhmanova A, Miedema K, Hennig W. Identification and characterization of the Drosophila histone H4 replacement gene. FEBS Letters. 1996 [accessed 2021 Dec 3];388(2–3):219–222. https://onlinelibrary.wiley.com/doi/full/10.1016/0014-5793%2896%2900551-0. doi:10.1016/0014-5793(96)00551-0

4. Armstrong RL, Penke TJR, Chao SK, Gentile GM, Strahl BD, Matera AG, McKay DJ, Duronio RJ. H3K9 Promotes Under-Replication of Pericentromeric Heterochromatin in Drosophila Salivary Gland Polytene Chromosomes. Genes. 2019 [accessed 2022 Jan 5];10(2). /pmc/articles/PMC6409945/. doi:10.3390/GENES10020093

5. Armstrong RL, Penke TJR, Strahl BD, Matera AG, McKay DJ, MacAlpine DM, Duronio RJ. Chromatin conformation and transcriptional activity are permissive regulators of DNA replication initiation in Drosophila. Genome Research. 2018;28(11):1688–1700. doi:10.1101/gr.239913.118

6. Baker NE, Li K, Quiquand M, Ruggiero R, Wang LH. Eye development. Methods. 2014 [accessed 2020 Dec 12];68(1):252–259. /pmc/articles/PMC4073679/?report=abstract. doi:10.1016/j.ymeth.2014.04.007

7. Bateman JR, Larschan E, D'Souza R, Marshall LS, Dempsey KE, Johnson JE, Mellone BG, Kuroda MI. A Genome-Wide Screen Identifies Genes That Affect Somatic Homolog Pairing in Drosophila . G3: Genes|Genomes|Genetics. 2012;2(7):731–740. doi:10.1534/g3.112.002840

8. Beck DB, Burton A, Oda H, Ziegler-Birling C, Torres-Padilla M-E, Reinberg D. The role of PR-Set7 in replication licensing depends on Suv4-20h. Genes & development. 2012 [accessed 2019 Sep 17];26(23):2580–9. http://www.ncbi.nlm.nih.gov/pubmed/23152447. doi:10.1101/gad.195636.112

9. Beck DB, Oda H, Shen SS, Reinberg D. PR-set7 and H4K20me1: At the crossroads of genome integrity, cell cycle, chromosome condensation, and transcription. Genes and Development. 2012;26(4):325–337. doi:10.1101/gad.177444.111

10. Blazer LL, Lima-Fernandes E, Gibson E, Eram MS, Loppnau P, Arrowsmith CH, Schapira M, Vedadi M. PR Domain-containing Protein 7 (PRDM7) Is a Histone 3 Lysine 4 Trimethyltransferase. Journal of Biological Chemistry. 2016;291(26):13509–13519. doi:10.1074/JBC.M116.721472

11. Bodenhofer U, Bonatesta E, Horejš-Kainrath C, Hochreiter S. msa: an R package for multiple sequence alignment. Bioinformatics. 2015 [accessed 2021 Dec 3];31(24):3997–3999. https://academic.oup.com/bioinformatics/article/31/24/3997/197486. doi:10.1093/BIOINFORMATICS/BTV494

12. Botuyan MV, Lee J, Ward IM, Kim J-E, Thompson JR, Chen J, Mer G. Structural Basis for the Methylation State-Specific Recognition of Histone H4-K20 by 53BP1 and Crb2 in DNA Repair. Cell. 2006 [accessed 2019 Jun 7];127(7):1361–1373. https://www.sciencedirect.com/science/article/pii/S009286740601525X?via%3Dihub. doi:10.1016/J.CELL.2006.10.043

13. Brustel J, Kirstein N, Izard F, Grimaud C, Prorok P, Cayrou C, Schotta G, Abdelsamie AF, Déjardin J,

581 Méchali M, et al. Histone H4K20 tri-methylation at late-firing origins ensures timely heterochromatin
582 replication. The EMBO Journal. 2017;36(18):2726–2741. doi:10.15252/embj.201796541

583 14. Brustel J, Tardat M, Kirsh O, Grimaud C, Julien E. Coupling mitosis to DNA replication: The emerging
584 role of the histone H4-lysine 20 methyltransferase PR-Set7. Trends in Cell Biology. 2011;21(8):452–460.
585 doi:10.1016/j.tcb.2011.04.006

586 15. Brustel J, Tardat M, Kirsh O, Grimaud C, Julien E. Coupling mitosis to DNA replication: The emerging
587 role of the histone H4-lysine 20 methyltransferase PR-Set7. Trends in Cell Biology. 2011 [accessed 2019
588 Sep 24];21(8):452–460.
589 https://www.sciencedirect.com/science/article/pii/S0962892411000821?via%3Dihub.
590 doi:10.1016/J.TCB.2011.04.006

591 16. Centore RC, Havens CG, Manning AL, Li J-M, Flynn RL, Tse A, Jin J, Dyson NJ, Walter JC, Zou L.
592 CRL4Cdt2-Mediated Destruction of the Histone Methyltransferase Set8 Prevents Premature Chromatin
593 Compaction in S Phase. Molecular Cell. 2010 [accessed 2019 Jul 24];40(1):22–33.
594 https://www.sciencedirect.com/science/article/pii/S1097276510007434?via%3Dihub.
595 doi:10.1016/J.MOLCEL.2010.09.015

596 17. Congdon LM, Houston SI, Veerappan CS, Spektor TM, Rice JC. PR-Set7-mediated monomethylation of
597 histone H4 lysine 20 at specific genomic regions induces transcriptional repression. Journal of Cellular
598 Biochemistry. 2010;110(3):609–619. doi:10.1002/jcb.22570

599 18. Congdon LM, Sims JK, Tuzon CT, Rice JC. The PR-Set7 binding domain of Riz1 is required for the
600 H4K20me1-H3K9me1 trans-tail “histone code” and Riz1 tumor suppressor function. Nucleic Acids
601 Research. 2014;42(6):3580–3589. doi:10.1093/nar/gkt1377

602 19. Copur Ö, Gorchakov A, Finkl K, Kuroda MI, Müller J. Sex-specific phenotypes of histone H4 point
603 mutants establish dosage compensation as the critical function of H4K16 acetylation in Drosophila .
604 Proceedings of the National Academy of Sciences. 2018;115(52):13336–13341.
605 doi:10.1073/pnas.1817274115

606 20. Cornett EM, Ferry L, Defossez PA, Rothbart SB. Lysine Methylation Regulators Moonlighting outside
607 the Epigenome. Molecular Cell. 2019 [accessed 2020 Oct 1];75(6):1092–1101.
608 /pmc/articles/PMC6756181/?report=abstract. doi:10.1016/j.molcel.2019.08.026

609 21. D.A. Case, I.Y. Ben-Shalom, S.R. Brozell, D.S. Cerutti, T.E. Cheatham, III, V.W.D. Cruzeiro, T.A. Darden,
610 R.E. Duke, D. Ghoreishi, M.K. Gilson, H. Gohlke, A.W. Goetz, D. Greene, R Harris, N. Homeyer, Y. Huang,
611 S. Izadi, A. Kovalenko, T. Kurtzman, T.S. Lee DMY and PAK, Case DA, Walker RC, Cheatham TE,
612 Simmerling C, Roitberg A, Merz KM, Luo R, Darden T, D.A. Case, I.Y. Ben-Shalom, S.R. Brozell, D.S.
613 Cerutti, T.E. Cheatham, III, V.W.D. Cruzeiro, T.A. Darden, R.E. Duke, D. Ghoreishi, M.K. Gilson, H. Gohlke,
614 A.W. Goetz, D. Greene, R Harris, N. Homeyer, Y. Huang, S. Izadi, A. Kovalenko, T. Kurtzman, T.S. Lee DMY
615 and PAK, et al. Amber 2018. University of California, San Francisco. 2018. 2018:1–923.
616 http://ambermd.org/doc12/Amber18.pdf

617 22. Dhami GK, Liu H, Galka M, Voss C, Wei R, Muranko K, Kaneko T, Cregan SP, Li L, Li SS-C. Dynamic
618 Methylation of Numb by Set8 Regulates Its Binding to p53 and Apoptosis. Molecular Cell. 2013 [accessed
619 2019 Sep 24];50(4):565–576.
620 https://www.sciencedirect.com/science/article/pii/S109727651300333X?via%3Dihub.
621 doi:10.1016/J.MOLCEL.2013.04.028

622 23. Dhami GK, Liu H, Galka M, Voss C, Wei R, Muranko K, Kaneko T, Cregan SP, Li L, Li SSC. Dynamic

623 Methylation of Numb by Set8 Regulates Its Binding to p53 and Apoptosis. Molecular Cell.
624 2013;50(4):565–576. doi:10.1016/j.molcel.2013.04.028

625 24. Dillon SC, Zhang X, Trievel RC, Cheng X. The SET-domain protein superfamily: Protein lysine
626 methyltransferases. Genome Biology. 2005 [accessed 2021 Dec 6];6(8):1–10.
627 https://genomebiology.biomedcentral.com/articles/10.1186/gb-2005-6-8-227. doi:10.1186/GB-2005-6-
628 8-227/FIGURES/4

629 25. Dorighi KM, Swigut T, Henriques T, Bhanu N V., Scruggs BS, Nady N, Still CD, Garcia BA, Adelman K,
630 Wysocka J. Mll3 and Mll4 Facilitate Enhancer RNA Synthesis and Transcription from Promoters
631 Independently of H3K4 Monomethylation. Molecular Cell. 2017 [accessed 2020 Sep 23];66(4):568-
632 576.e4. /pmc/articles/PMC5662137/?report=abstract. doi:10.1016/j.molcel.2017.04.018

633 26. Dulev S, Tkach J, Lin S, Batada NN. SET 8 methyltransferase activity during the DNA double-strand
634 break response is required for recruitment of 53 BP 1 . EMBO reports. 2014;15(11):1163–1174.
635 doi:10.15252/embr.201439434

636 27. Fang J, Feng Q, Ketel CS, Wang H, Cao R, Xia L, Erdjument-Bromage H, Tempst P, Simon JA, Zhang Y.
637 Purification and Functional Characterization of SET8, a Nucleosomal Histone H4-Lysine 20-Specific
638 Methyltransferase not static. Dynamic changes in chromatin structure play important roles in many
639 biological processes, such as DNA replication, repair, reco. 2002.

640 28. Faragó A, Ürmösi A, Farkas A, Bodai L. The histone replacement gene His4r is involved in heat stress
641 induced chromatin rearrangement. Scientific Reports 2021 11:1. 2021 [accessed 2021 Dec 2];11(1):1–15.
642 https://www.nature.com/articles/s41598-021-84413-4. doi:10.1038/s41598-021-84413-4

643 29. Fumasoni I, Meani N, Rambaldi D, Scafetta G, Alcalay M, Ciccarelli FD. Family expansion and gene
644 rearrangements contributed to the functional specialization of PRDM genes in vertebrates. BMC
645 Evolutionary Biology 2007 7:1. 2007 [accessed 2021 Sep 20];7(1):1–11.
646 https://bmcecolevol.biomedcentral.com/articles/10.1186/1471-2148-7-187. doi:10.1186/1471-2148-7-
647 187

648 30. Götz AW, Williamson MJ, Xu D, Poole D, Le Grand S, Walker RC. Routine Microsecond
649 MolecularDynamics Simulationswith AMBER on GPUs. 1. Generalized Born. Journal of Chemical Theory
650 and Computation. 2012 [accessed 2022 Jan 4];8(5):1542. /pmc/articles/PMC3348677/.
651 doi:10.1021/CT200909J

652 31. Hamidi T, Singh AK, Veland N, Vemulapalli V, Chen J, Hardikar S, Bao J, Fry CJ, Yang V, Lee KA, et al.
653 Identification of Rpl29 as a major substrate of the lysine methyltransferase Set7/9. The Journal of
654 biological chemistry. 2018 [accessed 2022 Jan 5];293(33):12770–12780.
655 https://pubmed.ncbi.nlm.nih.gov/29959229/. doi:10.1074/JBC.RA118.002890

656 32. Hayashi-Takanaka Y, Hayashi Y, Hirano Y, Miyawaki-Kuwakado A, Ohkawa Y, Obuse C, Kimura H,
657 Haraguchi T, Hiraoka Y. Chromatin loading of MCM hexamers is associated with di-/tri-methylation of
658 histone H4K20 toward S phase entry. Nucleic Acids Research. 2021 [accessed 2022 Jan 4];49(21):12152–
659 12166. https://academic.oup.com/nar/article/49/21/12152/6426064. doi:10.1093/NAR/GKAB1068

660 33. Houston SI, McManus KJ, Adams MM, Sims JK, Carpenter PB, Hendzel MJ, Rice JC. Catalytic function
661 of the PR-Set7 histone H4 lysine 20 monomethyltransferase is essential for mitotic entry and genomic
662 stability. The Journal of biological chemistry. 2008 [accessed 2019 Jun 20];283(28):19478–88.
663 http://www.ncbi.nlm.nih.gov/pubmed/18480059. doi:10.1074/jbc.M710579200

664 34. Huen MSY, Sy SM-H, van Deursen JM, Chen J. Direct interaction between SET8 and proliferating cell
665 nuclear antigen couples H4-K20 methylation with DNA replication. The Journal of biological chemistry.
666 2008 [accessed 2019 Jun 7];283(17):11073–7. http://www.ncbi.nlm.nih.gov/pubmed/18319261.
667 doi:10.1074/jbc.C700242200

668 35. Jiang F, Liu Q, Wang Y, Zhang J, Wang H, Song T, Yang M, Wang X, Kang L. Comparative genomic
669 analysis of SET domain family reveals the origin, expansion, and putative function of the arthropod-
670 specific SmydA genes as histone modifiers in insects. GigaScience. 2017 [accessed 2021 Dec 6];6(6):1–
671 16. https://academic.oup.com/gigascience/article/6/6/gix031/3748233.
672 doi:10.1093/GIGASCIENCE/GIX031

673 36. Jørgensen S, Elvers I, Trelle MB, Menzel T, Eskildsen M, Jensen ON, Helleday T, Helin K, Sørensen CS.
674 The histone methyltransferase SET8 is required for S-phase progression. Journal of Cell Biology.
675 2007;179(7):1337–1345. doi:10.1083/jcb.200706150

676 37. Julien E, Herr W. A switch in mitotic histone H4 lysine 20 methylation status is linked to M phase
677 defects upon loss of HCF-1. Molecular Cell. 2004;14(6):713–725. doi:10.1016/j.molcel.2004.06.008

678 38. Kalakonda N, Fischle W, Boccuni P, Gurvich N, Hoya-Arias R, Zhao X, Miyata Y, MacGrogan D, Zhang J,
679 Sims JK, et al. Histone H4 lysine 20 monomethylation promotes transcriptional repression by L3MBTL1.
680 Oncogene. 2008 [accessed 2019 Jun 17];27(31):4293–4304.
681 http://www.nature.com/articles/onc200867. doi:10.1038/onc.2008.67

682 39. Kapoor-Vazirani P, Vertino PM. A dual role for the histone methyltransferase PR-SET7/SETD8 and
683 histone H4 lysine 20 monomethylation in the local regulation of RNA polymerase II pausing. Journal of
684 Biological Chemistry. 2014;289(11):7425–7437. doi:10.1074/jbc.M113.520783

685 40. Karachentsev D, Sarma K, Reinberg D, Steward R. PR-Set7-dependent methylation of histone H4 Lys
686 20 functions in repression of gene expression and is essential for mitosis. Genes and Development.
687 2005;19(4):431–435. doi:10.1101/gad.1263005

688 41. Leatham-Jensen M, Uyehara CM, Strahl BD, Matera AG, Duronio RJ, McKay DJ. Lysine 27 of
689 replication-independent histone H3.3 is required for Polycomb target gene silencing but not for gene
690 activation. PLOS Genetics. 2019 [accessed 2021 Sep 20];15(1):e1007932.
691 https://journals.plos.org/plosgenetics/article?id=10.1371/journal.pgen.1007932.
692 doi:10.1371/JOURNAL.PGEN.1007932

693 42. Li Y, Armstrong RL, Duronio RJ, Macalpine DM. Methylation of histone H4 lysine 20 by PR-Set7
694 ensures the integrity of late replicating sequence domains in Drosophila. Nucleic Acids Research.
695 2016;44(15):7204–7218. doi:10.1093/nar/gkw333

696 43. Li Y, Sun L, Zhang Y, Wang D, Wang F, Liang J, Gui B, Shang Y. The histone modifications governing
697 TFF1 transcription mediated by estrogen receptor. The Journal of biological chemistry. 2011 [accessed
698 2019 Aug 7];286(16):13925–36. http://www.ncbi.nlm.nih.gov/pubmed/21378170.
699 doi:10.1074/jbc.M111.223198

700 44. Li Z, Nie F, Wang S, Li L. Histone H4 Lys 20 monomethylation by histone methylase SET8 mediates
701 Wnt target gene activation. Proceedings of the National Academy of Sciences of the United States of
702 America. 2011;108(8):3116–3123. doi:10.1073/pnas.1009353108

703 45. Lukinović V, Casanova AG, Roth GS, Chuffart F, Reynoird N. Lysine Methyltransferases Signaling:
704 Histones are Just the Tip of the Iceberg. Current protein & peptide science. 2020 [accessed 2022 Jan

5];21(7):655–674. https://pubmed.ncbi.nlm.nih.gov/31894745/. doi:10.2174/1871527319666200102101608

46. Lv X, Han Z, Chen H, Yang B, Yang X, Xia Y, Pan C, Fu L, Zhang S, Han H, et al. A positive role for polycomb in transcriptional regulation via H4K20me1. Cell Research. 2016;26(5):529–542. doi:10.1038/cr.2016.33

47. Maier JA, Martinez C, Kasavajhala K, Wickstrom L, Hauser KE, Simmerling C. ff14SB: Improving the accuracy of protein side chain and backbone parameters from ff99SB. Journal of chemical theory and computation. 2015 [accessed 2022 Jan 4];11(8):3696. /pmc/articles/PMC4821407/. doi:10.1021/ACS.JCTC.5B00255

48. Manes G, Joly W, Guignard T, Smirnov V, Berthemy S, Bocquet B, Audo I, Zeitz C, Sahel J, Cazevieille C, et al. A novel duplication of PRMD13 causes North Carolina macular dystrophy: overexpression of PRDM13 orthologue in drosophila eye reproduces the human phenotype. Human Molecular Genetics. 2017 [accessed 2021 Sep 20];26(22):4367–4374. https://academic.oup.com/hmg/article/26/22/4367/4085843. doi:10.1093/HMG/DDX322

49. McKay DJ, Klusza S, Penke TJR, Meers MP, Curry KP, McDaniel SL, Malek PY, Cooper SW, Tatomer DC, Lieb JD, et al. Interrogating the function of metazoan histones using engineered gene clusters. Developmental Cell. 2015;32(3):373–386. doi:10.1016/j.devcel.2014.12.025

50. Meers MP, Adelman K, Duronio RJ, Strahl BD, McKay DJ, Matera AG. Transcription start site profiling uncovers divergent transcription and enhancer-associated RNAs in Drosophila melanogaster. BMC Genomics 2018 19:1. 2018 [accessed 2021 Sep 20];19(1):1–20. https://bmcgenomics.biomedcentral.com/articles/10.1186/s12864-018-4510-7. doi:10.1186/S12864-018-4510-7

51. Meers MP, Henriques T, Lavender CA, McKay DJ, Strahl BD, Duronio RJ, Adelman K, Matera AG. Histone gene replacement reveals a posttranscriptional role for H3K36 in maintaining metazoan transcriptome fidelity. eLife. 2017;6. doi:10.7554/ELIFE.23249

52. Meers MP, Leatham-Jensen M, Penke TJR, McKay DJ, Duronio RJ, Matera AG. An Animal Model for Genetic Analysis of Multi-Gene Families: Cloning and Transgenesis of Large Tandemly Repeated Histone Gene Clusters. Methods in Molecular Biology. 2018 [accessed 2021 Sep 20];1832:309–325. https://link.springer.com/protocol/10.1007/978-1-4939-8663-7_17. doi:10.1007/978-1-4939-8663-7_17

53. Meserve JH, Duronio RJ. A population of G2-arrested cells are selected as sensory organ precursors for the interommatidial bristles of the Drosophila eye. Developmental Biology. 2017;430(2):374–384. doi:10.1016/j.ydbio.2017.06.023

54. Milite C, Feoli A, Viviano M, Rescigno D, Cianciulli A, Balzano AL, Mai A, Castellano S, Sbardella G. The emerging role of lysine methyltransferase SETD8 in human diseases. Clinical Epigenetics. 2016;8(1). doi:10.1186/s13148-016-0268-4

55. Minakhina S, Steward R. Melanotic Mutants in Drosophila: Pathways and Phenotypes. Genetics. 2006 [accessed 2022 Jan 7];174(1):253–263. https://academic.oup.com/genetics/article/174/1/253/6061187. doi:10.1534/GENETICS.106.061978

56. Mis J, Ner SS, Grigliatti TA. Identification of three histone methyltransferases in Drosophila: dG9a is a suppressor of PEV and is required for gene silencing. Molecular Genetics and Genomics. 2006 [accessed 2021 Dec 6];275(6):513–526. https://link.springer.com/article/10.1007/s00438-006-0116-x.

746 doi:10.1007/S00438-006-0116-X/TABLES/2

747 57. Mohan M, Herz H-M, Smith ER, Zhang Y, Jackson J, Washburn MP, Florens L, Eissenberg JC,
748 Shilatifard A. The COMPASS Family of H3K4 Methylases in Drosophila. Molecular and Cellular Biology.
749 2011 [accessed 2021 Dec 6];31(21):4310–4318. https://journals.asm.org/doi/abs/10.1128/MCB.06092-
750 11. doi:10.1128/MCB.06092-11/ASSET/B99FA20A-F1B0-4422-BE8A-
751 927BA0E4090C/ASSETS/GRAPHIC/ZMB9991092610007.JPEG

752 58. Nakamura K, Saredi G, Becker JR, Foster BM, Nguyen N V., Beyer TE, Cesa LC, Faull PA, Lukauskas S,
753 Frimurer T, et al. H4K20me0 recognition by BRCA1–BARD1 directs homologous recombination to sister
754 chromatids. Nature Cell Biology. 2019;21(3):311–318. doi:10.1038/s41556-019-0282-9

755 59. Nikolaou KC, Moulos P, Chalepakis G, Hatzis P, Oda H, Reinberg D, Talianidis I. Spontaneous
756 development of hepatocellular carcinoma with cancer stem cell properties in PR-SET7-deficient livers.
757 The EMBO Journal. 2015;34(4):430–447. doi:10.15252/embj.201489279

758 60. Nishioka K, Chuikov S, Sarma K, Erdjument-Bromage H, Allis CD, Tempst P, Reinberg D. Set9, a novel
759 histone H3 methyltransferase that facilitates transcription by precluding histone tail modifications
760 required for heterochromatin formation. Genes and Development. 2002;16(4):479–489.
761 doi:10.1101/gad.967202

762 61. Nishioka K, Rice JC, Sarma K, Erdjument-Bromage H, Werner J, Wang Y, Chuikov S, Valenzuela P,
763 Tempst P, Steward R, et al. PR-Set7 is a nucleosome-specific methyltransferase that modifies lysine 20 of
764 histone H4 and is associated with silent chromatin. Molecular cell. 2002;9(6):1201–13.
765 http://www.ncbi.nlm.nih.gov/pubmed/12086618

766 62. Oda H, Hübner MR, Beck DB, Vermeulen M, Hurwitz J, Spector DL, Reinberg D. Regulation of the
767 Histone H4 Monomethylase PR-Set7 by CRL4Cdt2-Mediated PCNA-Dependent Degradation during DNA
768 Damage. Molecular Cell. 2010 [accessed 2019 Aug 5];40(3):364–376.
769 https://www.sciencedirect.com/science/article/pii/S1097276510007872?via%3Dihub

770 63. Oda H, Okamoto I, Murphy N, Chu J, Price SM, Shen MM, Torres-Padilla ME, Heard E, Reinberg D.
771 Monomethylation of Histone H4-Lysine 20 Is Involved in Chromosome Structure and Stability and Is
772 Essential for Mouse Development. Molecular and Cellular Biology. 2009;29(8):2278–2295.
773 http://mcb.asm.org/cgi/doi/10.1128/MCB.01768-08. doi:10.1128/MCB.01768-08

774 64. Pannetier M, Julien E, Schotta G, Tardat M, Sardet C, Jenuwein T, Feil R. PR-SET7 and SUV4-20H
775 regulate H4 lysine-20 methylation at imprinting control regions in the mouse. EMBO Reports.
776 2008;9(10):998–1005. doi:10.1038/embor.2008.147

777 65. Penke TJR, McKay DJ, Strahl BD, Matera AG, Duronio RJ. Direct interrogation of the role of H3K9 in
778 metazoan heterochromatin function. Genes & Development. 2016 [accessed 2021 Sep 20];30(16):1866–
779 1880. http://genesdev.cshlp.org/content/30/16/1866.full. doi:10.1101/GAD.286278.116

780 66. Penke TJR, McKay DJ, Strahl BD, Matera AG, Duronio RJ. Functional Redundancy of Variant and
781 Canonical Histone H3 Lysine 9 Modification in Drosophila. Genetics. 2018 [accessed 2021 Sep
782 20];208(1):229–244. https://academic.oup.com/genetics/article/208/1/229/6066502.
783 doi:10.1534/GENETICS.117.300480

784 67. Pesavento JJ, Yang H, Kelleher NL, Mizzen CA. Certain and Progressive Methylation of Histone H4 at
785 Lysine 20 during the Cell Cycle. Molecular and Cellular Biology. 2008;28(1):468–486.
786 doi:10.1128/mcb.01517-07

787 68. Rickels R, Herz HM, Sze CC, Cao K, Morgan MA, Collings CK, Gause M, Takahashi YH, Wang L,
788 Rendleman EJ, et al. Histone H3K4 monomethylation catalyzed by Trr and mammalian COMPASS-like
789 proteins at enhancers is dispensable for development and viability. Nature Genetics. 2017;49(11):1647–
790 1653. doi:10.1038/ng.3965

791 69. Rothbart SB, Strahl BD. Interpreting the language of histone and DNA modifications. Biochimica et
792 Biophysica Acta - Gene Regulatory Mechanisms. 2014;1839(8):627–643.
793 doi:10.1016/j.bbagrm.2014.03.001

794 70. Sakaguchi A, Joyce E, Aoki T, Schedl P, Steward R. The Histone H4 Lysine 20 Monomethyl Mark, Set
795 by PR-Set7 and Stabilized by L(3)mbt, Is Necessary for Proper Interphase Chromatin Organization. Imhof
796 A, editor. PLoS ONE. 2012 [accessed 2019 Aug 20];7(9):e45321.
797 https://dx.plos.org/10.1371/journal.pone.0045321. doi:10.1371/journal.pone.0045321

798 71. Sakaguchi A, Karachentsev D, Seth-Pasricha M, Druzhinina M, Steward R. Functional characterization
799 of the drosophila Hmt4-20/Suv4-20 histone methyltransferase. Genetics. 2008;179(1):317–322.
800 doi:10.1534/genetics.108.087650

801 72. Sakaguchi A, Steward R. Aberrant monomethylation of histone H4 lysine 20 activates the DNA
802 damage checkpoint in Drosophila melanogaster. Journal of Cell Biology. 2007;176(2):155–162.
803 doi:10.1083/jcb.200607178

804 73. Salomon-Ferrer R, Götz AW, Poole D, Le Grand S, Walker RC. Routine Microsecond Molecular
805 Dynamics Simulations with AMBER on GPUs. 2. Explicit Solvent Particle Mesh Ewald. Journal of chemical
806 theory and computation. 2013 [accessed 2022 Jan 4];9(9):3878–3888.
807 https://pubmed.ncbi.nlm.nih.gov/26592383/. doi:10.1021/CT400314Y

808 74. Schotta G, Lachner M, Sarma K, Ebert A, Sengupta R, Reuter G, Reinberg D, Jenuwein T. A silencing
809 pathway to induce H3-K9 and H4-K20 trimethylation at constitutive heterochromatin. Genes and
810 Development. 2004;18(11):1251–1262. doi:10.1101/gad.300704

811 75. Schotta G, Sengupta R, Kubicek S, Malin S, Kauer M, Callén E, Celeste A, Pagani M, Opravil S, De La
812 Rosa-Velazquez IA, et al. A chromatin-wide transition to H4K20 monomethylation impairs genome
813 integrity and programmed DNA rearrangements in the mouse. Genes & development. 2008 [accessed
814 2019 Sep 26];22(15):2048–61. http://www.ncbi.nlm.nih.gov/pubmed/18676810.
815 doi:10.1101/gad.476008

816 76. Shi X, Kachirskaia I, Yamaguchi H, West LE, Wen H, Wang EW, Dutta S, Appella E, Gozani O.
817 Modulation of p53 Function by SET8-Mediated Methylation at Lysine 382. Molecular Cell.
818 2007;27(4):636–646. doi:10.1016/j.molcel.2007.07.012

819 77. Shilatifard A. The COMPASS Family of Histone H3K4 Methylases: Mechanisms of Regulation in
820 Development and Disease Pathogenesis. http://dx.doi.org/10.1146/annurev-biochem-051710-134100.
821 2012 [accessed 2021 Dec 6];81:65–95. https://www.annualreviews.org/doi/abs/10.1146/annurev-
822 biochem-051710-134100. doi:10.1146/ANNUREV-BIOCHEM-051710-134100

823 78. Shoaib M, Chen Q, Shi X, Nair N, Prasanna C, Yang R, Walter D, Frederiksen KS, Einarsson H, Svensson
824 JP, et al. Histone H4 lysine 20 mono-methylation directly facilitates chromatin openness and promotes
825 transcription of housekeeping genes. Nature Communications 2021 12:1. 2021 [accessed 2021 Sep
826 29];12(1):1–16. https://www.nature.com/articles/s41467-021-25051-2. doi:10.1038/s41467-021-25051-
827 2

828 79. Shoaib M, Walter D, Gillespie PJ, Izard F, Fahrenkrog B, Lleres D, Lerdrup M, Johansen JV, Hansen K,
829 Julien E, et al. Histone H4K20 methylation mediated chromatin compaction threshold ensures genome
830 integrity by limiting DNA replication licensing. Nature Communications. 2018;9(1). doi:10.1038/s41467-
831 018-06066-8

832 80. Sims JK, Rice JC. PR-Set7 Establishes a Repressive trans-Tail Histone Code That Regulates
833 Differentiation. Molecular and Cellular Biology. 2008;28(14):4459–4468. doi:10.1128/mcb.00410-08

834 81. Spektor TM, Congdon LM, Veerappan CS, Rice JC. The UBC9 E2 sumo conjugating enzyme binds the
835 PR-Set7 histone methyltransferase to facilitate target gene repression. PLoS ONE. 2011;6(7).
836 doi:10.1371/journal.pone.0022785

837 82. Sugeedha J, Gautam J, Tyagi S. SET1/MLL family of proteins: functions beyond histone methylation.
838 Epigenetics. 2021 [accessed 2022 Jan 5];16(5):469–487. https://pubmed.ncbi.nlm.nih.gov/32795105/.
839 doi:10.1080/15592294.2020.1809873

840 83. Takawa M, Cho HS, Hayami S, Toyokawa G, Kogure M, Yamane Y, Iwai Y, Maejima K, Ueda K, Masuda
841 A, et al. Histone lysine methyltransferase setd8 promotes carcinogenesis by deregulating PCNA
842 expression. Cancer Research. 2012;72(13):3217–3227. doi:10.1158/0008-5472.CAN-11-3701

843 84. Tardat M, Brustel J, Kirsh O, Lefevbre C, Callanan M, Sardet C, Julien E. The histone H4 Lys 20
844 methyltransferase PR-Set7 regulates replication origins in mammalian cells. Nature Cell Biology.
845 2010;12(11):1086–1093. doi:10.1038/ncb2113

846 85. Tardat M, Brustel J, Kirsh O, Lefevbre C, Callanan M, Sardet C, Julien E. The histone H4 Lys 20
847 methyltransferase PR-Set7 regulates replication origins in mammalian cells. Nature Cell Biology.
848 2010;12(11):1086–1093. doi:10.1038/ncb2113

849 86. Tardat M, Murr R, Herceg Z, Sardet C, Julien E. PR-Set7-dependent lysine methylation ensures
850 genome replication and stability through S phase. Journal of Cell Biology. 2007;179(7):1413–1426.
851 doi:10.1083/jcb.200706179

852 87. Thandapani P, Couturier AM, Yu Z, Li X, Couture JF, Li S, Masson JY, Richard S. Lysine methylation of
853 FEN1 by SET7 is essential for its cellular response to replicative stress. Oncotarget. 2017 [accessed 2022
854 Jan 5];8(39):64918–64931. https://pubmed.ncbi.nlm.nih.gov/29029401/.
855 doi:10.18632/ONCOTARGET.18070

856 88. Tullio F Di, Schwarz M, Zorgati H, Mzoughi S, Guccione E. The duality of PRDM proteins: epigenetic
857 and structural perspectives. The FEBS Journal. 2021 [accessed 2021 Sep 20].
858 https://onlinelibrary.wiley.com/doi/full/10.1111/febs.15844. doi:10.1111/FEBS.15844

859 89. Wakabayashi K -i., Okamura M, Tsutsumi S, Nishikawa NS, Tanaka T, Sakakibara I, Kitakami J -i., Ihara
860 S, Hashimoto Y, Hamakubo T, et al. The Peroxisome Proliferator-Activated Receptor /Retinoid X
861 Receptor Heterodimer Targets the Histone Modification Enzyme PR-Set7/Setd8 Gene and Regulates
862 Adipogenesis through a Positive Feedback Loop. Molecular and Cellular Biology. 2009;29(13):3544–
863 3555. doi:10.1128/mcb.01856-08

864 90. Wakabayashi K, Okamura M, Tsutsumi S, Nishikawa NS, Tanaka T, Sakakibara I, Kitakami J, Ihara S,
865 Hashimoto Y, Hamakubo T, et al. The peroxisome proliferator-activated receptor gamma/retinoid X
866 receptor alpha heterodimer targets the histone modification enzyme PR-Set7/Setd8 gene and regulates
867 adipogenesis through a positive feedback loop. Molecular and cellular biology. 2009 [accessed 2019 Jun
868 28];29(13):3544–55. http://www.ncbi.nlm.nih.gov/pubmed/19414603. doi:10.1128/MCB.01856-08

869 91. Wang H, Cao R, Xia L, Erdjument-Bromage H, Borchers C, Tempst P, Zhang Y. Purification and
870 Functional Characterization of a Histone H3-Lysine 4-Specific Methyltransferase. Molecular Cell.
871 2001;8(6):1207–1217. doi:10.1016/S1097-2765(01)00405-1

872 92. Weirich S, Kudithipudi S, Jeltsch A. Specificity of the SUV4-20H1 and SUV4-20H2 protein lysine
873 methyltransferases and methylation of novel substrates. Journal of Molecular Biology.
874 2016;428(11):2344–2358. doi:10.1016/j.jmb.2016.04.015

875 93. West LE, Roy S, Lachmi-Weiner K, Hayashi R, Shi X, Appella E, Kutateladze TG, Gozani O. The MBT
876 repeats of L3MBTL1 link SET8-mediated p53 methylation at lysine 382 to target gene repression. Journal
877 of Biological Chemistry. 2010;285(48):37725–37732. doi:10.1074/jbc.M110.139527

878 94. Wolff T, Ready DF. The beginning of pattern formation in the Drosophila compound eye: The
879 morphogenetic furrow and the second mitotic wave. Development. 1991;113(3):841–850.

880 95. Wu S, Rice JC. A new regulator of the cell cycle: The PR-Set7 histone methyltransferase. Cell Cycle.
881 2011;10(1):68–72. doi:10.4161/cc.10.1.14363

882 96. Wu S, Wang W, Kong X, Congdon LM, Yokomori K, Kirschner MW, Rice JC. Dynamic regulation of the
883 PR-Set7 histone methyltransferase is required for normal cell cycle progression. Genes and
884 Development. 2010;24(22):2531–2542. doi:10.1101/gad.1984210

885 97. Yang F, Sun L, Li Q, Han X, Lei L, Zhang H, Shang Y. SET8 promotes epithelial-mesenchymal transition
886 and confers TWIST dual transcriptional activities. The EMBO Journal. 2012 [accessed 2019 Aug
887 8];31(1):110–123. http://emboj.embopress.org/cgi/doi/10.1038/emboj.2011.364.
888 doi:10.1038/emboj.2011.364

889 98. Yang H, Pesavento JJ, Starnes TW, Cryderman DE, Wallrath LL, Kelleher NL, Mizzen CA. Preferential
890 dimethylation of histone H4 lysine 20 by Suv4-20. Journal of Biological Chemistry. 2008;283(18):12085–
891 12092. doi:10.1074/jbc.M707974200

892 99. Yao L, Li Y, Du F, Han X, Li X, Niu Y, Ren S, Sun Y. Histone H4 Lys 20 methyltransferase SET8 promotes
893 androgen receptor-mediated transcription activation in prostate cancer. Biochemical and Biophysical
894 Research Communications. 2014 [accessed 2019 Nov 20];450(1):692–696.
895 https://linkinghub.elsevier.com/retrieve/pii/S0006291X14011073. doi:10.1016/j.bbrc.2014.06.033

896 100. Yin L, Yu VC, Zhu G, Chang DC. SET8 plays a role in controlling G1/S transition by blocking lysine
897 acetylation in histone through binding to H4 N-terminal tail. Cell Cycle. 2008;7(10):1423–1432.
898 doi:10.4161/cc.7.10.5867

899 101. Yu G. Using ggtree to Visualize Data on Tree-Like Structures. Current Protocols in Bioinformatics.
900 2020 [accessed 2021 Dec 3];69(1):e96. https://onlinelibrary.wiley.com/doi/full/10.1002/cpbi.96.
901 doi:10.1002/CPBI.96

902 102. Yu G, Lam TTY, Zhu H, Guan Y. Two Methods for Mapping and Visualizing Associated Data on
903 Phylogeny Using Ggtree. Molecular Biology and Evolution. 2018 [accessed 2021 Dec 3];35(12):3041–
904 3043. https://academic.oup.com/mbe/article/35/12/3041/5142656. doi:10.1093/MOLBEV/MSY194

905 103. Yu G, Smith DK, Zhu H, Guan Y, Lam TTY. ggtree: an r package for visualization and annotation of
906 phylogenetic trees with their covariates and other associated data. Methods in Ecology and Evolution.
907 2017 [accessed 2021 Dec 3];8(1):28–36. https://onlinelibrary.wiley.com/doi/full/10.1111/2041-
908 210X.12628. doi:10.1111/2041-210X.12628

909 104. Yu N, Huangyang P, Yang X, Han X, Yan R, Jia H, Shang Y, Sun L. microRNA-7 Suppresses the Invasive
910 Potential of Breast Cancer Cells and Sensitizes Cells to DNA Damages by Targeting Histone
911 Methyltransferase SET8. Journal of Biological Chemistry. 2013 [accessed 2019 Nov 20];288(27):19633–
912 19642. http://www.jbc.org/lookup/doi/10.1074/jbc.M113.475657. doi:10.1074/jbc.M113.475657

913 105. Yu Y, Liu L, Li X, Hu X, Song H. The histone H4K20 methyltransferase PR-Set7 fine-tunes the
914 transcriptional activation of Wingless signaling in Drosophila. Journal of Genetics and Genomics.
915 2019;46(1):57–59. doi:10.1016/j.jgg.2018.06.009

916 106. Zhang J, Hou W, Chai M, Zhao H, Jia J, Sun X, Zhao B, Wang R. MicroRNA-127-3p inhibits
917 proliferation and invasion by targeting SETD8 in human osteosarcoma cells. Biochemical and Biophysical
918 Research Communications. 2016 [accessed 2019 Nov 20];469(4):1006–1011.
919 https://linkinghub.elsevier.com/retrieve/pii/S0006291X1531072X. doi:10.1016/j.bbrc.2015.12.067

920 107. Zhang X, Huang Y, Shi X. Emerging roles of lysine methylation on non-histone proteins. Cellular and
921 molecular life sciences : CMLS. 2015 [accessed 2022 Jan 5];72(22):4257–4272.
922 https://pubmed.ncbi.nlm.nih.gov/26227335/. doi:10.1007/S00018-015-2001-4

923 108. Zouaz A, Fernando C, Perez Y, Sardet C, Julien E, Grimaud C. Cell-cycle regulation of non-enzymatic
924 functions of the Drosophila methyltransferase PR-Set7. Nucleic Acids Research. 2018;46(6):2834–2849.
925 doi:10.1093/nar/gky034

926

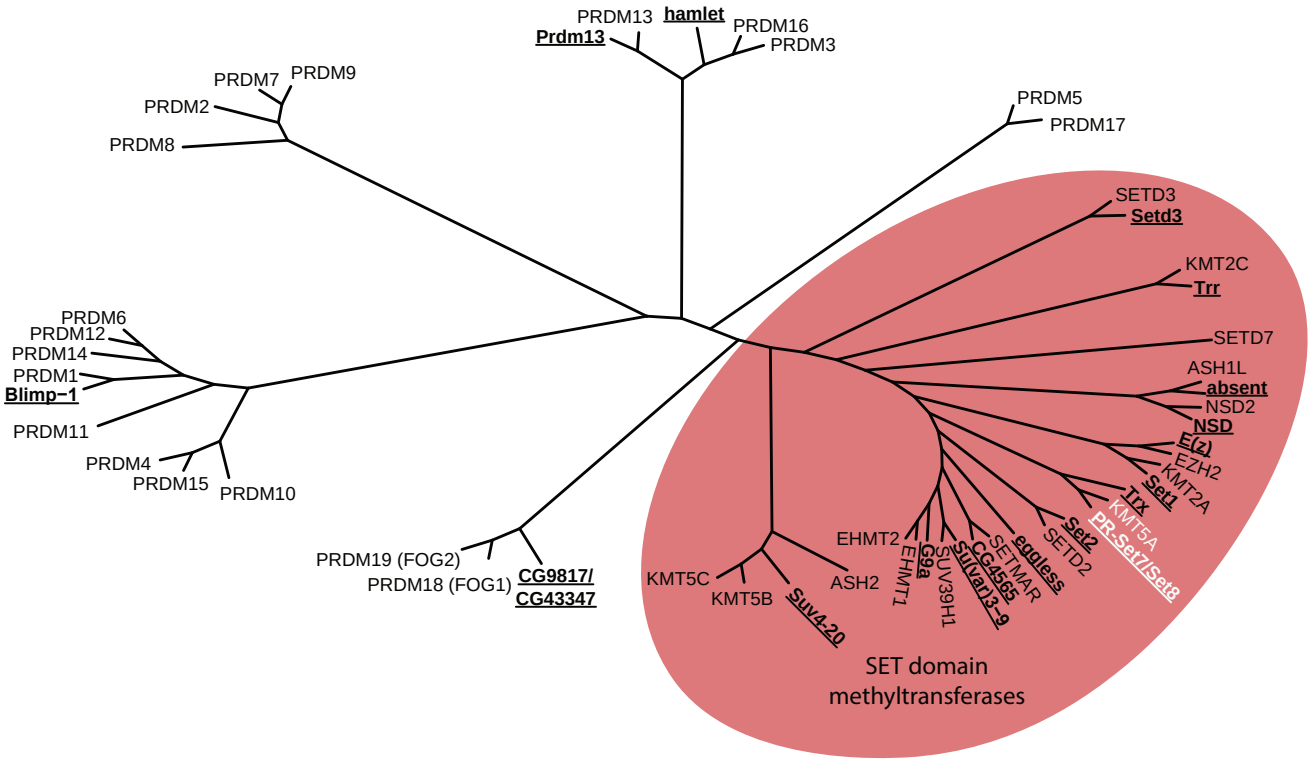

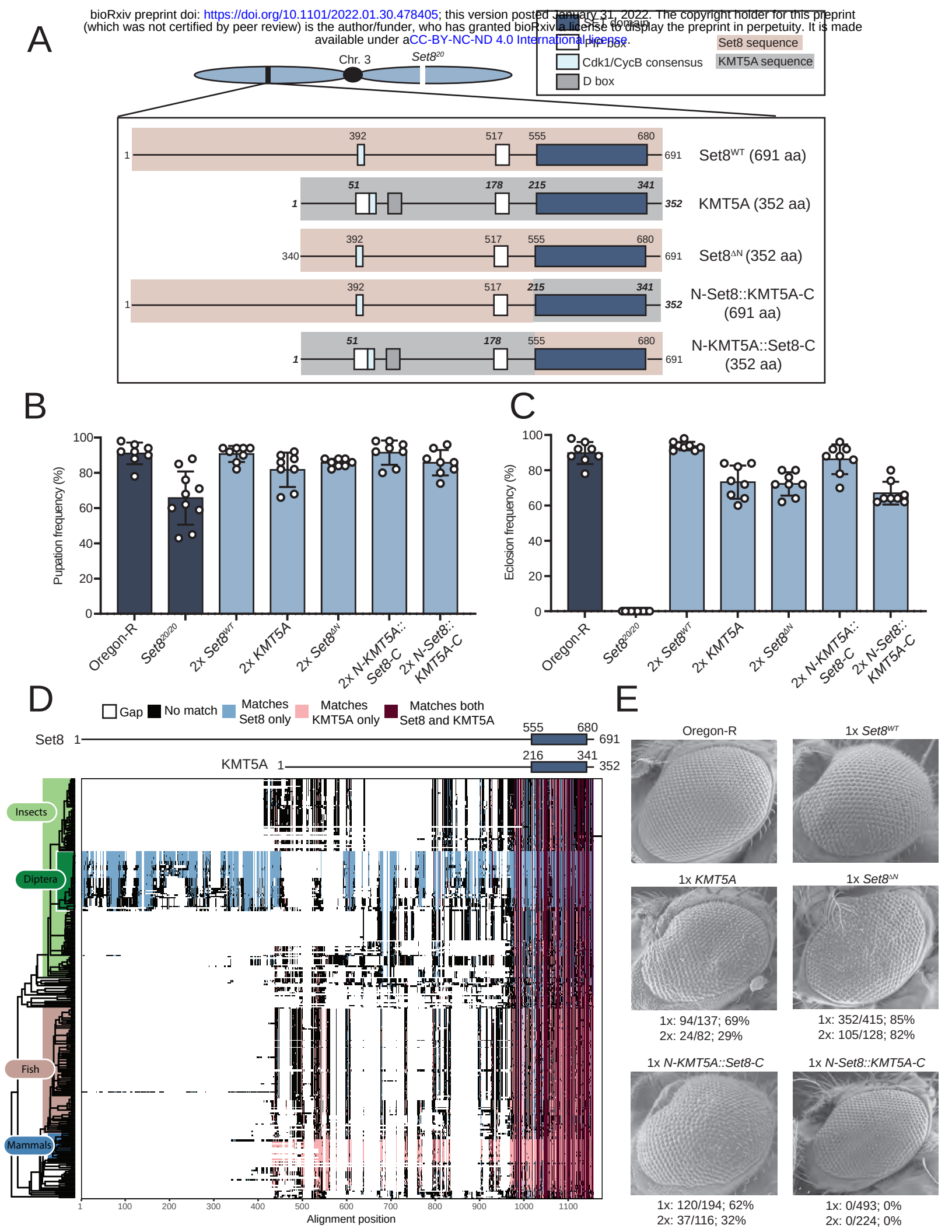

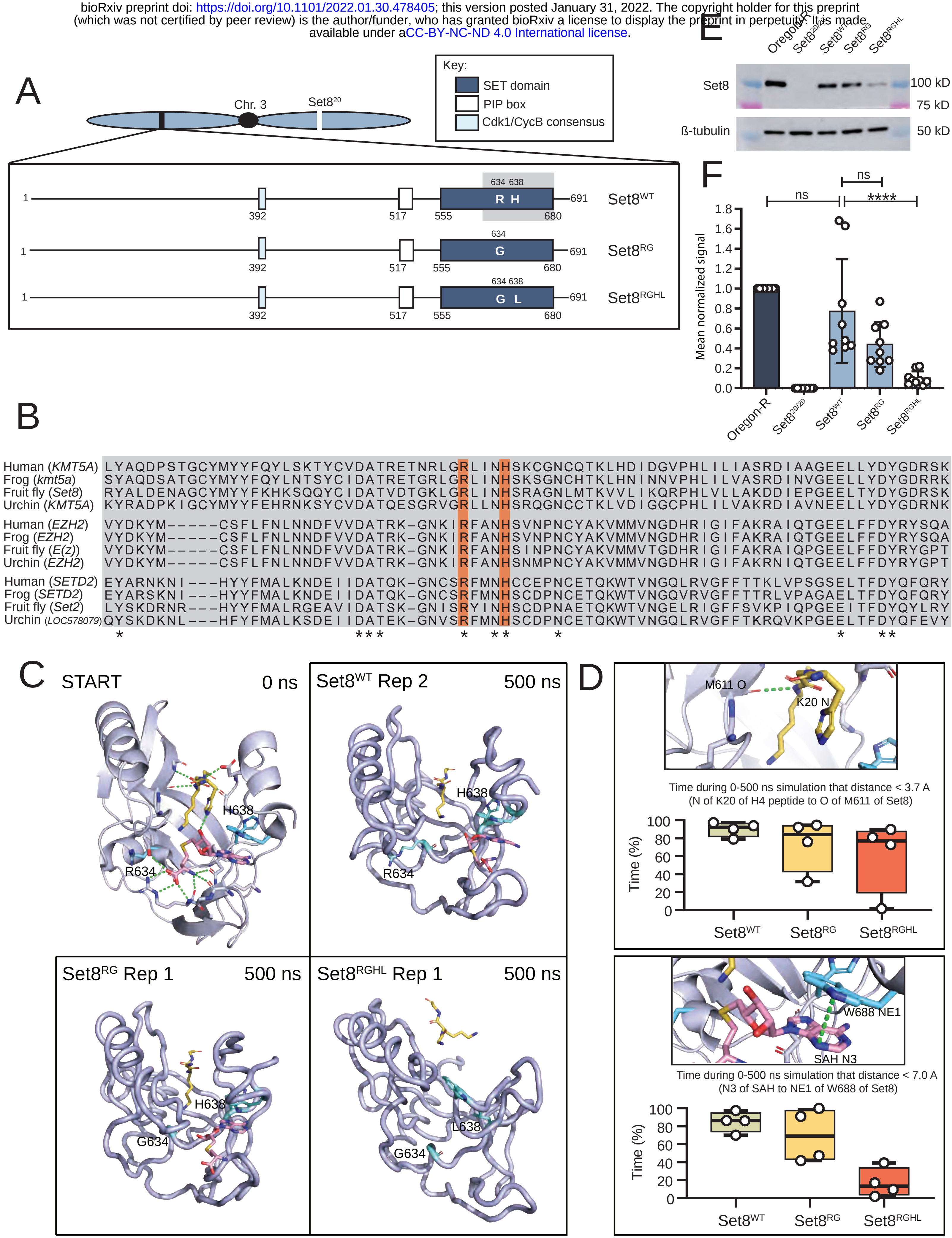

A

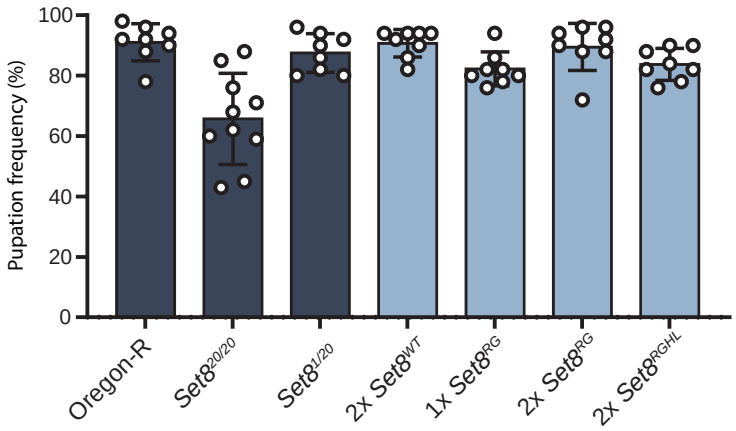

B

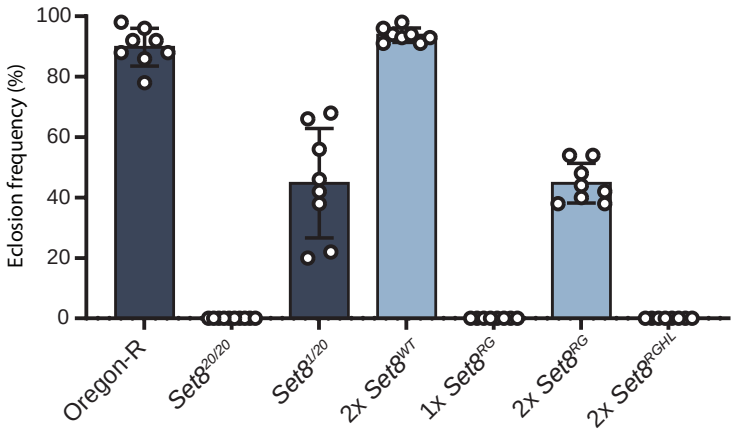

C

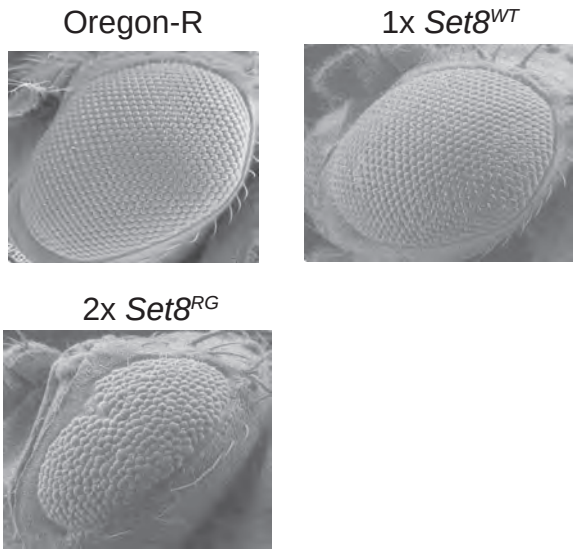

2x: 32/37; 86%

D